Supporting Information

Cooperative Atomic Mechanism of Emergent Tilted Magnetic Anisotropy

Brajagopal Das, Cinthia Piamonteze, Lior Kornblum*

Brajagopal Das, Lior Kornblum

Andrew & Erna Viterbi Department of Electrical & Computer Engineering, Technion Israel Institute of Technology, Haifa 3200003, Israel

E-mail: brajagopal.technion@gmail.com

Cinthia Piamonteze

Center for Photon Science, Paul Scherrer Institute, 5232, Villigen PSI, Switzerland

Structural characterization of the 10%Ru-LSMO films

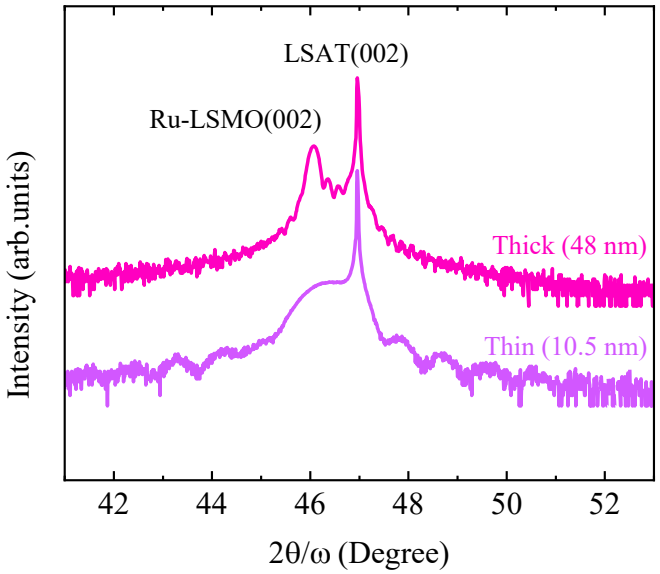

Figure S1. X-ray diffraction (2θ/ω) scans of 10% Ru-LSMO films around their pseudo-cubic (002) reflections (data adapted from our previous work[1]). The (002) Bragg peak of the thick (48 nm) and thin (10.5 nm) 10% Ru-LSMO films, together with that of the LSAT substrate, are shown in the figure, respectively. The sharp peak and clear Laue oscillations confirm the high structural quality of the epitaxial films. The extracted tetragonality (c/a ~ 1.02, where c is the out-of-plane and a the in-plane lattice parameter), arising from substrate-induced compressive strain, is later used to estimate the strength of single-ion anisotropy in Ru ions.

Background correction of the Ru-$M_{2,3}$ and Mn-$L_{2,3}$ spectra

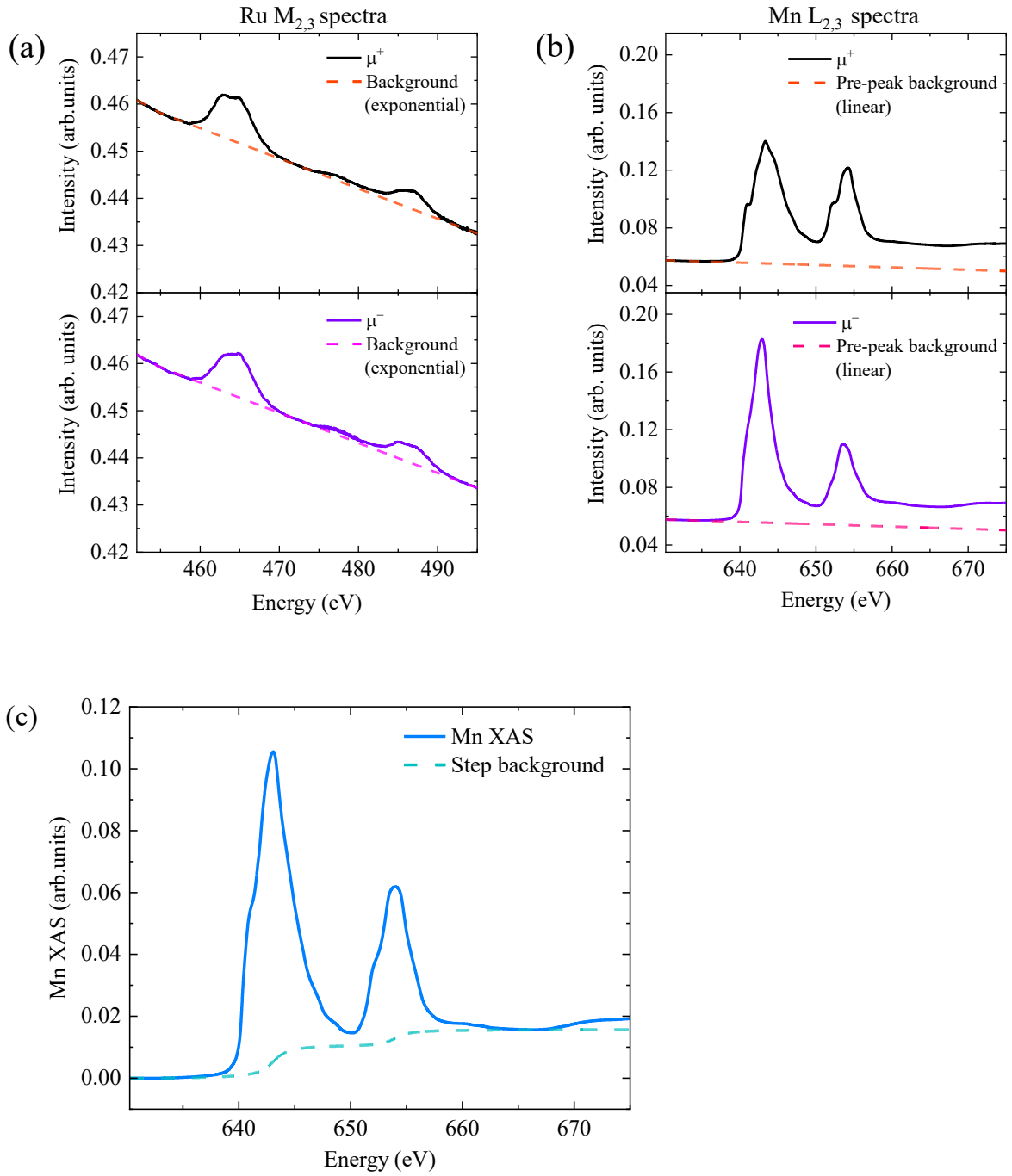

Figure S2. (a) Ru $M_{2,3}$ spectra (solid curves, raw) with exponential (piecewise) background (dashed curves, fitted), and (b) Mn $L_{2,3}$ spectra (solid curves, raw) with pre-peak linear background (dashed curves, fitted) for right (μ^+) and left (μ^-) circularly polarized x-rays. (c) Mn XAS plot with edge jumps at the $L_{2,3}$ edges, where XAS is defined as the average of intensities I(μ^+) and I(μ^-), after pre-peak linear background correction. All the measurements were performed at 30K.

The shape of the raw Ru $M_{2,3}$ spectra and the fitted background for Ru $M_{2,3}$ spectra agree well with the earlier XMCD study of Ru ions in Ru-LSMO films.[2] The Ru $M_{2,3}$ spectra with intensities $I(\mu^+)$ and $I(\mu^-)$ were obtained after the exponential background subtraction. These spectra were subsequently used for calculating XMCD $(I(\mu^+) - I(\mu^-))$ and XAS $([I(\mu^+) + I(\mu^-)]/2)$. For Mn $L_{2,3}$ spectra, pre-peak linear background has been fitted and then the straight line has been extrapolated well beyond the L_2 edge. After the linear background subtraction, the Mn $L_{2,3}$ spectra of $I(\mu^+)$ and $I(\mu^-)$ were used for XMCD and XAS. To apply the orbital and spin sum rules, the edge jump background with the jumps at the Mn L_3 and L_2 edges was subtracted from Mn XAS, as described elsewhere.[3] The procedure of background subtraction for Ru and Mn ions explained here is for [001] direction of the thick Ru-LSMO film; however, the same procedures were applied to the other directions of both the thick and thin 10%Ru-LSMO films. The XAS and XMCD spectra are then normalized by the corresponding total absorption (XAS area) along each crystallographic direction, meaning normalized $\mathrm{XAS} = \mathrm{XAS}/(\mathrm{XAS\ area})$ and normalized $\mathrm{XMCD} = \mathrm{XMCD}/(\mathrm{XAS\ area})$.

Element specific magnetic anisotropy in the thin (10.5nm) 10%Ru-LSMO film

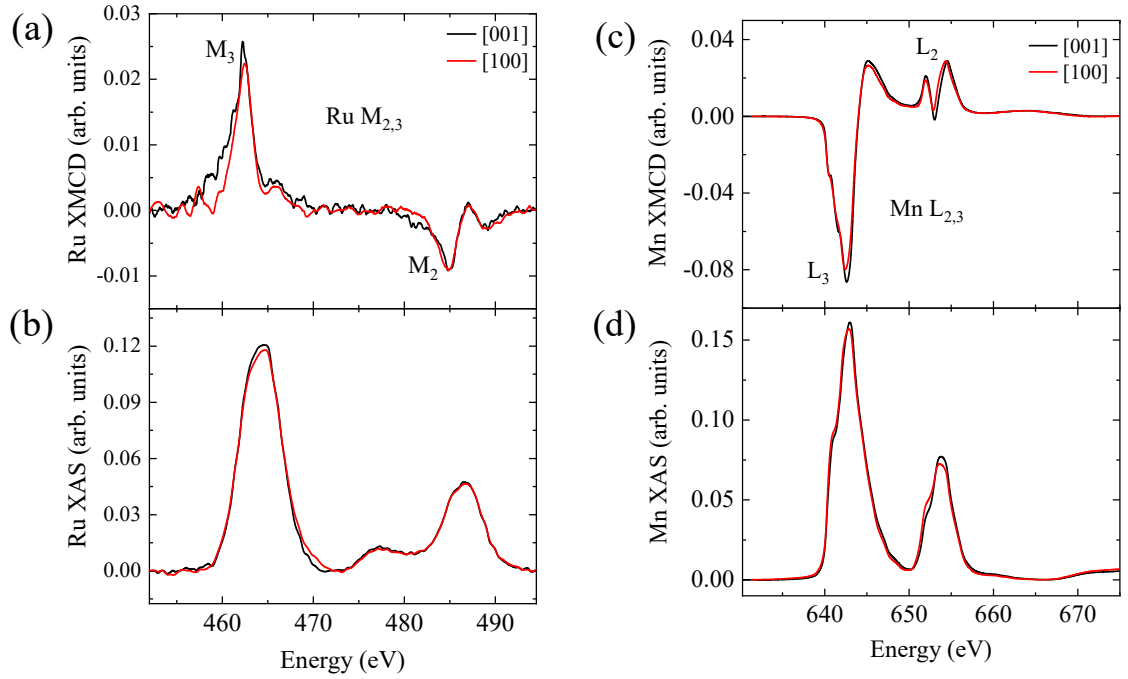

Figure S3. Normalized Ru $M_{2,3}$-edge (a) XMCD and (b) XAS of the thin (10.5 nm) 10%Ru-LSMO film along the pseudo-cubic directions [001] and [100]. Normalized Mn $L_{2,3}$-edge (c) XMCD and (d) XAS of the thin 10%Ru-LSMO film.

The normalized XMCD and XAS spectra of Ru and Mn of the thin Ru-LSMO film are presented in Figure S3. We note three key features in these spectra: First, the Ru XMCD spectra indicate tilted magnetic anisotropy (TMA) in the Ru ions (Figure S3a), with the Ru M_3 peak of the out-of-plane (OOP) direction [001] being noticeably larger than that of the in-plane direction [100] at high field (5T), while the M_2 peak remains nearly unchanged with angle (discussed below). Second, the Mn XMCD spectra (Figure S3c) are almost identical along these directions, indicating the magnetically isotropic behavior of the Mn ions at high field. Third, the positive (negative) Ru-M_3 (M_2) XMCD peak and negative (positive) Mn-L_3 (L_2) peak confirm that Ru ions are antiferromagnetically coupled with the Mn ions, in agreement with a previous observation,[2] and theoretical prediction.[4] In addition, we note a small Ru-XAS peak (Figure S3b) around 477eV, which is also observed in the thick Ru-LSMO film. This peak originates from the transition between 3p and 5s orbitals of the Ru ions, with no magnetic contribution as observed in the XMCD spectra (Figure S3a).[5] Finally, it is worth noting that the Ru M_2 peak is insensitive to angular change, owing to the restricted set of dipole-allowed transitions at the M_2 edge, which makes this feature intrinsically less responsive to angular variation, while any small differences can be readily masked by baseline effects.[6]

Table S1. Orbital (m_{orb}) moments and effective spin ($m_{spin,eff}$) moments of Ru and Mn ions for [001] and [100] directions of the thin 10%Ru-LSMO film. The values were calculated using the sum rules; all the units are in Bohr magneton per atom.

	[001]	[100]
$m^{Ru}_{spin,eff}$	-0.94 ± 0.02	-0.75 ± 0.02
m^{Ru}_{orb}	-0.25 ± 0.03	-0.15 ± 0.02
m^{Ru}_{total}	-1.19 ± 0.05	-0.90 ± 0.04
$m^{Ru}_{orb}/m^{Ru}_{spin,eff}$	0.27	0.20
$m^{Mn}_{spin,eff}$	3.2 ± 0.04	3.16 ± 0.03
m^{Mn}_{orb}	-0.01 ± 0.01	-0.01 ± 0.01
m^{Mn}_{total}	3.19 ± 0.05	3.15 ± 0.04
$m^{Mn}_{orb}/m^{Mn}_{spin,eff}$	0.0	0.0

The results of the sum rules are summarized in Table S1. The key result is anisotropic behavior of orbital-to-spin moment ratio $\left(m_{orb}^{Ru}/m_{spin,eff}^{Ru}\right)$ in Ru ions, confirming the presence of Ru single-ion anisotropy. We note that the orbital-to-spin moment ratio for [100] direction is significantly higher in the thin Ru-LSMO film compared to that of the thick film. This discrepancy originates from the in-plane symmetry breaking (Figure S5, Table S2) in the thick film. Furthermore, the Mn ions exhibit no single-ion anisotropy, consistent with the results from thick film.

To estimate the strength of TMA in Ru ions of the thin Ru-LSMO film, we compare the strain state and structural parameters (c/a ratio) of our films with those of well-established $SrRuO_3$ (SRO) films, where single-ion of Ru ions drives macroscopic magnetic anisotropy. The relevant parameters, particularly strain, octahedral tilt pattern, and out-of-plane to in-plane lattice parameter ratio, which critically influence single-ion anisotropy, are found to be comparable in both the systems.[1,7,8] In the epitaxial SRO films, the strength of TMA has been reported to be in the order of 10^6 J.m^{-3}.[6,7] Taking into account the structural similarity, strain conditions and diluted concentration (10%) of Ru ions, we estimate the strength of TMA in Ru-LSMO to be an order of 10^5 J.m^{-3}. This suggests that the strength of TMA in Ru ions is comparable with that of the macroscopic TMA, which is 4×10^5 J·m^{-3}, calculated from macroscopic magnetization data acquired from the thin Ru-LSMO film reported in our previous work,[1] using a standard method of estimating effective magnetic anisotropy energy from the area between the [001] and [100] M–H loops in the first quadrant.[9] This supports our microscopic observation that Ru ions drive the macroscopic anisotropy in Ru-LSMO. This interpretation is consistent with previous macroscopic studies.[1,4,10]

While the Mn ions exhibit isotropic magnetization (Figure S3c and Table S1) at high field (5T) due to their fully aligned isotropic spin moments, a closer look at the magnetic field-dependent behavior (Figure S4) reveals the presence of TMA in Mn ions at lower fields, where perpendicular magnetization is stronger than in-plane magnetization. The XMCD hysteresis loops of the Mn ions show that TMA exists up to a threshold field of $\sim \pm 2.5$ T, with a strength of 1.1×10^5 J·m^{-3}. This strength is comparable with the estimated strength of TMA in Ru ions. This suggests that the Mn ions, despite their weak SOC and lack of single-ion anisotropy, also play a crucial role in stabilizing the macroscopic magnetic anisotropy in Ru-LSMO.

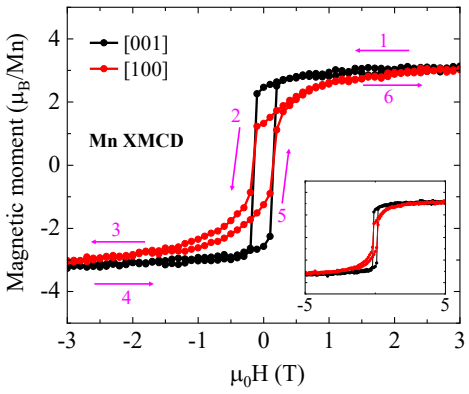

Figure S4. Magnetic field dependence of Mn XMCD along the [001] and [100] directions of the thin 10%Ru-LSMO film; the XMCD hysteresis loops are scaled using the Mn spin moments obtained from the sum rule analysis. The pink arrows indicate the sweeping direction, and the inset shows the full sweep range up to 5T.

In-plane symmetry breaking in the thick 10%Ru-LSMO film

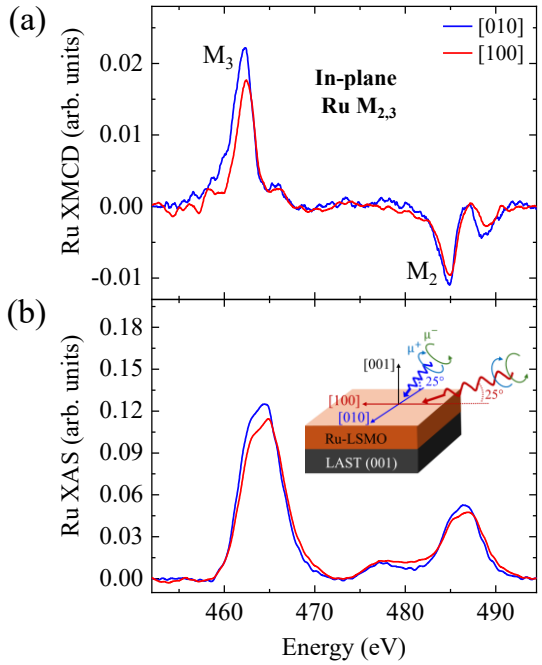

Figure S5. Normalized Ru $M_{2,3}$-edge (a) XMCD and (b) XAS of the thick (48 nm) 10%Ru-LSMO film along the in-plane pseudo-cubic directions [010] and [100]. A schematic of the measurement axes is depicted in the inset.

As demonstrated in our previous work, 1D periodic structural modulation emerges in Ru-LSMO films above a critical thickness due to shear strain relaxation, resulting in significantly

anisotropic in-plane magnetization.[1] The in-plane structural symmetry breaking creates anisotropic bonding environment, which is expected to introduce anisotropic orbital moments, anisotropic spin moments, and anisotropic orbital-to-spin moment ratio in Ru ions through strong SOC of Ru ions.[11] This effect is precisely observed in the in-pane XMCD spectra of Ru ions (Figure S5 and Table S2). These results suggest that Ru ions are not only responsible for the emergence of TMA but also plays the key role in driving anisotropic in-plane magnetization.

Table S2. Orbital (m_{orb}) moments and effective spin ($m_{spin,eff}$) moments of Ru and Mn ions for [010] and [100] directions of the thick 10%Ru-LSMO film. The values were calculated using the sum rules; all the units are in Bohr magneton per atom.

	[010]	[100]
$m^{Ru}_{spin,eff}$	-0.85 ± 0.02	-0.69 ± 0.02
m^{Ru}_{orb}	-0.17 ± 0.02	-0.08 ± 0.01
m^{Ru}_{total}	-1.02 ± 0.04	-0.77 ± 0.03
$m^{Ru}_{orb}/m^{Ru}_{spin,eff}$	0.2	0.12

References

[1] B. Das, L. Wysocki, J. Schöpf, et al., "Tilted Magnetic Anisotropy with In-Plane Broken Symmetry in Ru-Substituted Manganite Films," *Advanced Electronic Materials* **2023**, *9*, 2300253. https://doi.org/10.1002/aelm.202300253.

[2] T. Harano, G. Shibata, K. Ishigami, et al., "Role of doped Ru in coercivity-enhanced $La_{0.6}Sr_{0.4}MnO_3$ thin film studied by x-ray magnetic circular dichroism," *Applied Physics Letters* **2013**, *102*, 222404. https://doi.org/10.1063/1.4808090.

[3] J. Grabis, A. Bergmann, A. Nefedov, K. Westerholt, H. Zabel, "Element-specific x-ray circular magnetic dichroism of Co_2MnGe Heusler thin films," *Physical Review B* **2005**, *72*, 24437. https://doi.org/10.1103/PhysRevB.72.024437.

[4] E. Hua, L. Si, K. Dai, et al., "Ru-Doping-Induced Spin Frustration and Enhancement of the Room-Temperature Anomalous Hall Effect in $La_{2/3}Sr_{1/3}MnO_3$ Films," *Advanced Materials* **2022**, *34*, 2206685. https://doi.org/10.1002/adma.202206685.

[5] Y. K. Wakabayashi, M. Kobayashi, Y. Takeda, et al., "Isotropic orbital magnetic moments in magnetically anisotropic $SrRuO_3$ films," *Physical Review Materials* **2022**, *6*, 94402. https://doi.org/10.1103/PhysRevMaterials.6.094402.

[6] V. N. Antonov, D. A. Kukusta, "Electronic structure and x-ray magnetic circular dichroism in the multiferroic oxide h-$YbFeO_3$," *Physical Review B* **2019**, *99*, 104403. https://doi.org/10.1103/PhysRevB.99.104403.

[7] H. Wang, G. Laskin, W. He, et al., "Tunable Magnetic Anisotropy in Patterned $SrRuO_3$ Quantum Structures: Competition between Lattice Anisotropy and Oxygen Octahedral Rotation," *Advanced Functional Materials* **2022**, *32*, 2108475. https://doi.org/10.1002/adfm.202108475.

[8] W. Lu, W. Dong Song, K. He, et al., "The role of octahedral tilting in the structural phase transition and magnetic anisotropy in $SrRuO_3$ thin film," *Journal of Applied Physics* **2013**, *113*, 63901. https://doi.org/10.1063/1.4790699.

[9] D. Yi, C. L. Flint, P. P. Balakrishnan, et al., "Tuning Perpendicular Magnetic Anisotropy by Oxygen Octahedral Rotations in $(La_{1-x}Sr_xMnO_3)/(SrIrO_3)$ Superlattices," *Physical Review Letters* **2017**, *119*, 77201. https://doi.org/10.1103/PhysRevLett.119.077201.

[10] M. Nakamura, D. Morikawa, X. Yu, et al., "Emergence of topological hall effect in half-metallic manganite thin films by tuning perpendicular magnetic anisotropy," *Journal of the Physical Society of Japan* **2018**, *87*, 1. https://doi.org/10.7566/JPSJ.87.074704.

[11] J. Stöhr, "Exploring the microscopic origin of magnetic anisotropies with X-ray magnetic circular dichroism (XMCD) spectroscopy," *Journal of Magnetism and Magnetic Materials* **1999**, *200*, 470. https://doi.org/10.1016/S0304-8853(99)00407-2.